High Resolution Scan Mode SAR Using Compressive Sensing

Liu, D.; Boufounos, P.T.

TR2013-124 September 2013

Abstract

Conventional scan-mode synthetic aperture radar (SAR) covers a large area at the expense of reduced azimuth resolution, compared to other operation modes. In this paper, we develop a high resolution scan-mode SAR using random steering and compressive sensing (CS) based techniques. Our approach randomizes the beam steering pattern of conventional scan-mode SAR in both azimuth and range directions such that each pulse beam illuminates a different, randomly chosen, part of the area of interest. We model the image to be reconstructed as a combination of a sparse and a dense component, and combine sparse recovery with least squares methods to estimate them. Our experimental results demonstrate that the proposed randomly steered scan-mode SAR can improve imaging resolution without compromising the covered area size.

Asia-Pacific Conference on Synthetic Aperture Radar

High Resolution Scan Mode SAR Using Compressive Sensing

Dehong Liu, Petros T. Boufounos
Mitsubishi Electric Research Labs
{liudh, petrosb}@merl.com

***Abstract*—Conventional scan-mode synthetic aperture radar (SAR) covers a large area at the expense of reduced azimuth resolution, compared to other operation modes. In this paper, we develop a high resolution scan-mode SAR using random steering and compressive sensing (CS) based techniques. Our approach randomizes the beam steering pattern of conventional scan-mode SAR in both azimuth and range directions such that each pulse beam illuminates a different, randomly chosen, part of the area of interest. We model the image to be reconstructed as a combination of a sparse and a dense component, and combine sparse recovery with least squares methods to estimate them. Our experimental results demonstrate that the proposed randomly steered scan-mode SAR can improve imaging resolution without compromising the covered area size.**

I. INTRODUCTION

Monostatic Synthetic Aperture Radar (SAR) systems exhibit a tradeoff between imaging resolution and ground area coverage. For example, stripmap-mode SAR images a long swath by keeping the antenna pointed to a fixed direction as the platform moves along the SAR path. In contrast, spotlight-mode SAR images a much smaller area at much higher resolution by steering the antenna to always point to and illuminate the same spot in the ground. The trade-off between the two can be adjusted using sliding spotlight-mode SAR [1], [2]. An area larger than in stripmap-mode can be imaged using scan-mode SAR, in which the antenna is periodically steered to scan spots of different swaths, yielding a large multi-swath area at the cost of much lower azimuth resolution. With large coverage it is difficult, but very desirable, to achieve high resolution in a conventional SAR with a single pass observation.

The development of compressive sensing (CS) and its application to radar [3], [4] can be used to improve this trade-off. Using CS-based theory and methods, signals can be reconstructed robustly using fewer measurements than their Nyquist sampling rate. In SAR systems, this translates to significant coverage or resolution improvements. For example, our earlier work on stripmap, spotlight and sliding spotlight modes enables significant increase in the area covered without compromising resolution or, alternatively, significant increase in resolution without compromising range coverage [5]–[7].

In this paper, we extend and generalize our earlier work to scan mode SAR, aiming to increase the imaging resolution while maintaining its large coverage using CS-based techniques. In [5], [7] we consider random steering along the azimuth direction to improve coverage in spotlight mode or increase the resolution in sliding spotlight mode. The system we develop in this paper further uses steering along the ranges direction, i.e., exploits two steering dimensions instead of one. Thus, the randomly steered beam can now illuminate multi-swath areas and flexible shapes. The randomly steered antenna achieves a larger effective aperture for each point in the imaged area, compared to typical scan mode SAR. Using CS-based signal models and algorithms we can reconstruct the image from the acquired data at the, much higher, resolution corresponding to the larger effective aperture.

Compared to conventional scan mode SAR, our radar operation only differs in the antenna steering. The antenna of conventional scan mode SAR is steerable in the range direction and able to illuminate different swaths. Our radar platform requires additional flexibility to steer in both range and azimuth directions. At each pulse transmission the antenna is steered randomly such that the beam illuminates a spot randomly located uniformly within the large area of interest. The randomization, which can be pre-designed, ensures the measurements capture sufficient information to reconstruct a high resolution image using CS-based methods. It also enables irregular image shapes, impossible with conventional modes. Due to space limitations, this flexibility is not explored here.

Although our radar platform requires more steering flexibility, it provides higher imaging resolution than conventional scan mode. In conventional scan-mode SAR, images are reconstructed separately for each different swath and stitched together to generate a multi-swath image of a large area. In our high resolution scan mode, instead, imaging of the whole area is treated as an inverse problem. The imaged area is reconstructed as a whole using data collected from randomly distributed spots, properly taking into account the leakage from the sidelobes of each beam. The randomization yields a significantly larger effective aperture compared to conventional scan mode and, therefore, significantly higher resolution.

In this paper we mainly focus on the CS-based reconstruction algorithm, assuming uniformly random beam steering. Since SAR images exhibit limited sparsity, our approach decomposes the underlying SAR image into a sparse and a dense component. We first reconstruct the sparse component using a sparse recovery algorithm. Then we obtain a least-squares estimate of the dense component from the residual data. The sum of the components is the reconstructed ground reflectivity. Our experiments showed that our hybrid model outperforms CS algorithms that only perform sparse recovery.

The next section describes our proposed steering mode,

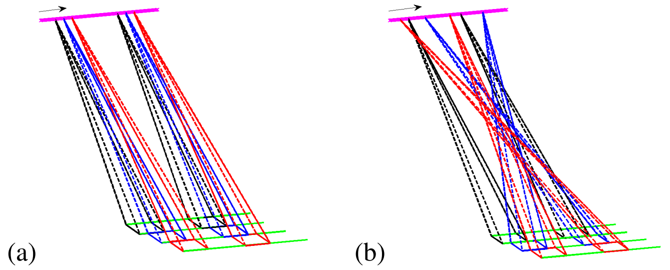

Fig. 1. Beam steering: (a) conventional and (b) randomly-steered scan mode.

as well as the computational model for its implementation. Section III presents the reconstruction algorithm. In Section IV we validate the performance improvements of our approach, compared to conventional scan mode SAR, in simulation. Section V discusses our results and concludes.

II. MODEL OF SCAN MODE SAR

We consider radar imaging using a linear mono-static synthetic array. To image an area, a mobile radar platform moves along a linear path, transmitting pulses at a uniform rate and recording their reflections from the area of interest. Each reflection is effectively a convolution of the transmitted pulse with the reflectivity of the illuminated area. We model conventional spotlight-mode acquisition as a linear operation:

$$\mathbf{y} = \mathbf{\Phi}\mathbf{x} + \mathbf{n}, \tag{1}$$

where $\mathbf{y}$ denotes the received radar echoes, $\mathbf{x}$ denotes the reflectivity of the imaged area, $\mathbf{\Phi}$ models the array acquisition function, and $\mathbf{n}$ is measurement noise.

Scan-mode SAR enables imaging of much wider area, at the expense of azimuth resolution. Scan mode, in contrast to spotlight mode, steers each pulse to a different spot. Specifically, the antenna is periodically steered in the range direction such that each burst of pulses illuminates adjacent swaths sequentially, at the same azimuth direction, as illustrated in Fig. 1(a). The result is wider swath coverage compared to other SAR modes. However, each point in the measured scene is illuminated at lower pulse repetition frequency (PRF) compared to strip-map SAR, thus reducing the azimuth resolution. At the processing stage, each range subswath is handled separately, forming a low resolution image. These images are stitched together to produce the final wide-swath image. Such wide swaths are impossible to image using other SAR modes.

Our CS-based high-resolution scan SAR system operates similarly to conventional SAR in uniformly transmitting pulses and receiving echoes, but differs in antenna steering, as illustrated in Fig. 1(b). Instead of steering the antenna to sequentially illuminate spots at different swaths, as conventional scan-mode SAR does, we steer the antenna in both azimuth and range directions and illuminate spots picked randomly within the area of interest, with equal probability. Each spot has the same size as that of a single spot in a conventional spotlight SAR system. The randomized steering schedule, which can be pre-designed, ensures the measurements capture enough information for high resolution image reconstruction.

To model the acquisition we start with the conventional spotlight mode model in (1). In this model, we consider the large area to be imaged as a whole and denote it using $\mathbf{v}$. At the i^{th} pulse transmission, where $i = 1, ..., N$ for N total pulses, the antenna is steered according to the steering schedule, effectively windowing $\mathbf{v}$ with an illumination beampattern, the spatial effect of which we denote using $\mathbf{W}_i$. Thus the area illuminated is equal to $\mathbf{x}_i = \mathbf{W}_i\mathbf{v}$. Note that $\mathbf{W}_i$ also captures detailed beampattern characteristics, such as the sidelobes.

To implement the system transfer function and obtain the i^{th} received echo, we first presume that the same window shape $\mathbf{W}_i$ is used for all pulses, i.e., the system operates in conventional spotlight mode without steering. Using (1) we then obtain the complete received data for that spot, denoted $\mathbf{y}_i = \mathbf{\Phi}\mathbf{x}_i$, where Φ is implemented using a fast algorithm, such as the wave-number algorithm [2]. Since we are only interested in the i^{th} received echo, we can select it from the data $\mathbf{y}_i$; we use $\mathbf{E}_i$ to denote this selection operator. Putting everything together, the i^{th} echo is obtained using $\mathbf{E}_i\mathbf{\Phi}\mathbf{W}_i\mathbf{v}$. Thus, the received data, denoted $\mathbf{u}$, is acquired as

$$\mathbf{u} = \begin{bmatrix} \mathbf{E}_1\mathbf{y}_1 \\ \vdots \\ \mathbf{E}_N\mathbf{y}_N \end{bmatrix} = \begin{bmatrix} \mathbf{E}_1\mathbf{\Phi}\mathbf{W}_1 \\ \vdots \\ \mathbf{E}_N\mathbf{\Phi}\mathbf{W}_N \end{bmatrix} \mathbf{v} = \mathbf{\Psi}\mathbf{v}. \tag{2}$$

By modifying the window $\mathbf{W}_i$ in (2) according to the steering schedule we can model conventional scan mode, the mode proposed in this paper, as well as a variety of other operation modes. For example, in conventional scan mode, the spot described by $\mathbf{W}_i$ periodically shifts spatially in azimuth and sequentially in range, thus scanning the whole area. In the proposed randomly steered scan mode, the spot of $\mathbf{W}_i$ is distributed uniformly at random in the whole imaging area. Of course, to reduce computational complexity, we select each $\mathbf{W}_i$ from a discrete set of pre-determined overlapping spatial windows distributed uniformly in the area of interest.

Since each point in the scene is illuminated from several distant positions in the radar path, the effective aperture looking at each point is the whole path of the platform, similar to conventional spotlight mode. In contrast, conventional scan mode illuminates each point only in part of the radar path, i.e., at smaller effective aperture, making azimuth resolution much smaller. This aperture gain is limited. As the scene becomes larger, all else being equal, each point is illuminated by fewer pulses, i.e., is measured less. Thus, the same number of measurements are used to recover a larger scene. Reconstruction is only possible if the scene is sparser or, generally, exhibits more structure. The exploitable scene structure determines the potential resolution improvement over scan mode.

III. CS BASED IMAGE RECONSTRUCTION

As described above, once the randomized steering of the array beam is determined, the resulting acquisition can be modeled using the linear system in (2). However, in contrast to conventional SAR systems, the system described by $\mathbf{\Psi}$ is underdetermined. In other words, inverting the system is not straightforward and can only be performed accurately using prior information on the signal.

Conventional CS methods regularize the reconstruction using sparsity of the acquired signal $\mathbf{v}$, in some domain, as a prior. Unfortunately, radar images are not very sparse in this sense. While they contain strong components in some domain, they also contain a significant residual that sparse methods do not consider. Thus, we propose a CS-based algorithm that, instead of only recovering a sparse signal, decomposes $\mathbf{v}$ into a sparse part $\mathbf{v}_s$ and a dense residual $\mathbf{v}_r$ [5], [7]:

$$\mathbf{v} = \mathbf{v}_s + \mathbf{v}_r. \tag{3}$$

Of course, the measured data can be notionally separated to $\mathbf{u} = \mathbf{\Psi}\mathbf{v}_s + \mathbf{\Psi}\mathbf{v}_r$ by substituting (3) into (2). Treating $\mathbf{u}_r = \mathbf{\Psi}\mathbf{v}_r$ as noise, our approach first computes an estimate of the sparse signal component $\mathbf{v}_s$ using standard CS-based methods:

$$\widehat{\mathbf{v}}_s = \arg\min_{\mathbf{v}} ||\mathbf{u} - \mathbf{\Psi}\mathbf{v}||_2^2 \quad \text{s.t.} \quad \|\mathbf{v}\|_0 < T. \tag{4}$$

Using the sparse estimate we compute the residual due to the dense component, i.e., $\widehat{\mathbf{u}}_r = \mathbf{u} - \mathbf{\Psi}\widehat{\mathbf{v}}_s$. The dense component can then be estimated using least squares:

$$\widehat{\mathbf{v}}_r = \mathbf{\Psi}^\dagger(\mathbf{u} - \mathbf{\Psi}\widehat{\mathbf{v}}_s). \tag{5}$$

The final image is the sum of the two estimates, (4) and (5).

The algorithm in Fig. 2 efficiently implements this idea. First the residual is initialized from the measurements, i.e., $\mathbf{u}_r^{(0)} = \mathbf{u}$, with $\widehat{\mathbf{v}}_s^{(0)} = \mathbf{0}$. Each iteration uses the residual $\mathbf{u}_r^{(k-1)}$ estimate the so-far unexplained signal $\tilde{\mathbf{v}}^{(k)}$. A threshold $\tau^{(k)}$ separating the large reflectors is computed as a fraction of the largest in magnitude component. After hard thresholding, $\mathcal{H}_{\tau^{(k)}}(\tilde{\mathbf{v}}^{(k)})$, i.e., setting all components less than $\tau^{(k)}$ in magnitude to zero, the strongest reflectors are estimated in $\mathbf{d}^{(k)}$. This estimate is scaled, using $\beta^{(k)}$, to capture most of the residual energy in $\mathbf{u}_r^{(k-1)}$, and added to the overall signal estimate from the previous iteration $\widehat{\mathbf{v}}_s^{(k-1)}$ to produce the current signal estimate $\widehat{\mathbf{v}}_s^{(k)}$. The residual $\mathbf{u}_r^{(k-1)}$ is updated and the algorithm iterates. After K iterations, with K sufficiently large to capture the strongest reflectors, we combine the final sparse estimate $\widehat{\mathbf{v}}_s^{(K)}$ with the least squares estimate of the dense component, $\mathbf{\Psi}^\dagger\mathbf{u}_r^{(K)}$, to produce the final image $\widehat{\mathbf{v}}$.

Our experiments demonstrated that this hybrid approach, in which the final image is composed of a sparse and a dense component, outperformed approaches using only sparse regularization. Of course, the dense component can only be estimated subject to the nullspace of the measurement operator $\mathbf{\Psi}$. However, this estimate is better than ignoring its presence, typically done in sparse methods. Our experiments showed that $\alpha > 0.5$ is a good choice for imaging performance.

For efficient implementation, a fast algorithm such as the wave-number algorithm should be used to approximate $\mathbf{\Phi}$ and its inversion [2]. Thus, using simple efficient implementations of the diagonal operators $\mathbf{E}_i$ and $\mathbf{W}_i$, we can implement $\mathbf{\Psi} = \mathbf{E}\mathbf{\Phi}\mathbf{W}$ as described in (2). Of course, as the number of possible steering spots increases, this implementation approach becomes increasingly inefficient since we need to compute one instance of the wave-number algorithm for each spot. A more efficient implementation is necessary but not explored here.

```
1) Initialize $0 < \alpha < 1$, $\widehat{\mathbf{v}}_s^{(0)} = \mathbf{0}$, $\mathbf{u}_r^{(0)} = \mathbf{u}$,
2) FOR $k = 1 : K$
       $\tilde{\mathbf{v}}^{(k)} = \mathbf{\Psi}^\dagger \mathbf{u}_r^{(k-1)}$
       $\tau^{(k)} = \max(|\tilde{\mathbf{v}}^{(k)}|) \cdot \alpha$
       $\mathbf{d}^{(k)} = \mathcal{H}_{\tau^{(k)}}(\tilde{\mathbf{v}}^{(k)})$
       $\tilde{\mathbf{u}}^{(k)} = \mathbf{\Psi}\mathbf{d}^{(k)}$
       $\beta^{(k)} = \frac{< \tilde{\mathbf{u}}^{(k)}, \mathbf{u}_r^{(k-1)} >}{< \tilde{\mathbf{u}}^{(k)}, \tilde{\mathbf{u}}^{(k)} >}$
       $\mathbf{u}_r^{(k)} = \mathbf{u}_r^{(k-1)} - \beta^{(k)}\tilde{\mathbf{u}}^{(k)}$
       $\widehat{\mathbf{v}}_s^{(k)} = \widehat{\mathbf{v}}_s^{(k-1)} + \beta^{(k)}\mathbf{d}^{(k)}$
   END
3) Output
       Image: $\widehat{\mathbf{v}} = \widehat{\mathbf{v}}_s^{(K)} + \mathbf{\Psi}^\dagger \mathbf{u}_r^{(K)}$
```

Fig. 2. Reconstruction algorithm

IV. EXPERIMENTS

To validate our approach, we simulate the SAR acquisition and reconstruction on an area with complex-valued ground reflectivity using both a conventional scan SAR and the proposed system. In the simulations we use a typical ground reflectivity image, representative of typical SAR images, which contains man-made and natural structures.

We partition the area of interest into a total number of 120 overlapping rectangular spots, along 8×15 range-azimuth grids. In conventional scan mode SAR, we divide the whole virtual aperture into 120 sub apertures correspondingly, with each sub-aperture illuminating each spot with a burst of multiple pulses, scanning the spots sequentially within the area of interest. Depending on the overlap, the effective aperture for each ground point can be larger than the size of a single sub aperture, but still less than the full synthetic aperture. For example, if there is no overlap, the effective aperture will be the same as a single sub aperture and the imaged area size is the largest possible. If all spots fully overlap, the operation is equivalent to spotlight mode and the effective aperture will be the same as the full synthetic aperture and the imaged area size is the smallest possible, i.e., the same as the size of the spot. Thus, controlling the overlap trades-off coverage with effective aperture size, i.e., resolution.

For the proposed randomly steered scan SAR, we predesign a steering pattern such that each spot is illuminated randomly with uniform probability. Thus, each point in the ground receives a small fraction of transmitting pulses across the full synthetic aperture, depending on the random steering and spot overlapping. Thus the effective aperture is the same as the synthetic aperture and the area covered is controlled by the overlap, as above. As described earlier, the trade-off here is that a scene with more structure is required in larger areas.

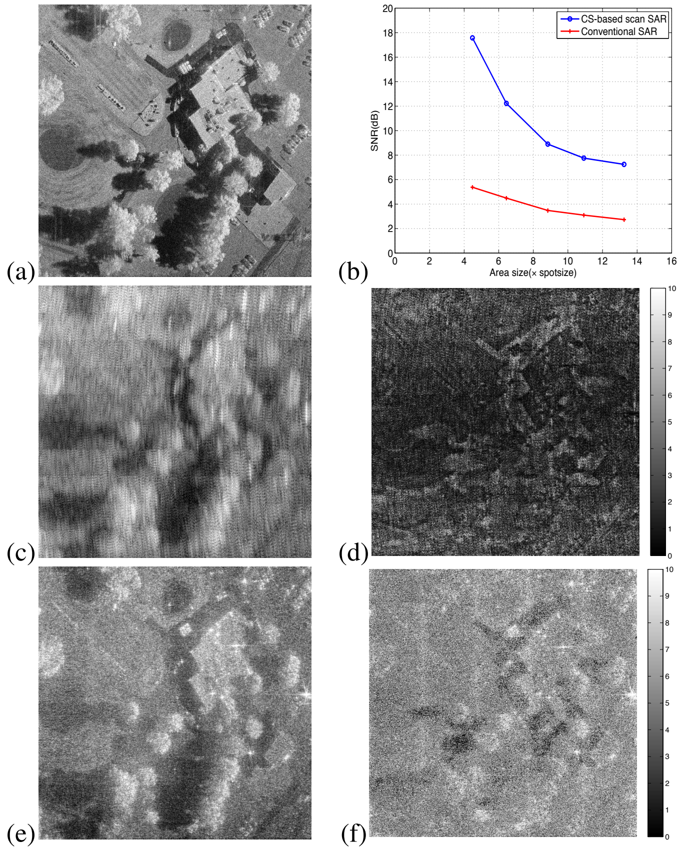

Fig. 3. (a) True ground reflectivity. (b) SNR of both modes as a function of area size. (c) Imaging and (d) point-wise SNR using classical scan mode SAR. (e) Imaging and (f) point-wise SNR using randomly steerable SAR.

Fig. 3(a) plots the magnitude of the true complex-valued ground reflectivity of the imaged area. Fig. 3(c) plots the conventional scan mode imaging result and Fig. 3(e) plots the reconstructed image using the randomly steered scan mode.

As evident by comparing Fig. 3(c) with Fig. 3(e), the reconstructed image using the randomized acquisition is much sharper compared to scan mode. The fine structures in the ground are significantly less blurred and fine details are discernible. As we describe above, this is due to the larger effective aperture of the randomly steered mode compared to the scan mode. Thus, using the signal model, our algorithm is able to exploit the structure of the image by identifying the strong reflectors and reconstructing them at much higher resolution. Since these are the dominant components, the resulting image reconstruction performance is improved.

To quantify the image resolution improvement, we compute the point-wise reconstruction SNR for both modes, and plot it in Fig. 3(d) and (f) for classical and randomized scan mode, respectively. The SNR of the classical scan mode is significantly lower. Furthermore, the performance is much worse in strong scatterers, which are smeared by the blurring due to the lower resolution. In contrast, the randomized scan mode exhibits significantly better SNR, especially in strong scattering areas. This is expected as the reconstruction algorithm prioritizes strong scatterers, reconstructing them first, before estimating regions with lower reflectivity.

To compare the SNR improvement for different coverage, we adjust the overlap between spots such that the SAR systems can cover different area size. For comparison, Fig. 3(b) plots the mean SNRs as a function of the coverage size, measured with as a multiple of the size of a single spot. As the scan area becomes larger, both the SNR and the SNR improvement due to our approach decreases. This is because as the coverage increases, fewer measurements are collected from each spot, and CS-based reconstruction becomes more difficult, especially when the underlying signal is not very sparse. Still, the proposed approach performs better than conventional scan mode.

In terms of computational complexity, we should note that our proposed approach is significantly heavier than conventional methods due to the iterative reconstruction. This holds even with the help of fast imaging algorithm such as the wavenumber algorithm. It is, therefore, necessary to improve our computational efficiency for the future work to enhance our high-resolution scan SAR capabilities.

V. CONCLUSION

Our work demonstrates that appropriate use of CS-based techniques can significantly improve the resolution of scan SAR systems, without compromise in the covered area. Specifically, randomizing the antenna steering increases the effective aperture of the radar and exploiting the partial sparsity of the image enables high-resolution reconstruction.

While we have demonstrated significant improvements, we also note that the reconstruction requires heavy computation. However, there is significant scope and opportunity for improvement, especially in implementing the forward and adjoint operators derived by random steering. These operators are integral to the performance of any iterative reconstruction algorithm necessary to implement such systems.

REFERENCES

[1] I. G. Cumming and F. H. Wong, *Digital processing of synthetic aperture radar data: algorithms and implementation*, Artech House, 2005.

[2] W. G. Carrara, R. S. Goodman, and R. M. Majewski, *Spotlight Synthetic Aperture Radar - Signal Processing Algorithms*, Artech House, 1995.

[3] R. Baraniuk and P. Steeghs, "Compressive radar imaging," in *IEEE Radar Conference*, MA, April 2007.

[4] L. C. Potter, E. Ertin, J. T. Parker, and M. Cetin, "Sparsity and compressed sensing in radar imaging," *Processings of the IEEE*, vol. 98, pp. 1006–1020, June 2010.

[5] D. Liu and P. T. Boufounos, "Random steerable arrays for synthetic aperture imaging," in *IEEE International conference on Acoustics Speech and Signal Processing(ICASSP)*, Canada, 2013.

[6] D. Liu and P. T. Boufounos, "High resolution SAR imaging using random pulse timing," in *IEEE International Geoscience and Remote Sensing Symposium (IGARSS)*, Canada, 2011.

[7] D. Liu and P. T. Boufounos, "Synthetic aperture imaging using a randomly steered spotlight," in *IEEE International Geoscience and Remote Sensing Symposium (IGARSS)*, Australia, 2013.